

# The Advanced Spectroscopic and Coronagraphic Explorer: science payload design concept

Larry D. Gardner, John L. Kohl, Peter S. Daigneau, Peter L. Smith, Leonard Strachan, Jr.  
Harvard-Smithsonian Center for Astrophysics, Cambridge MA 02138

Russell A. Howard, Dennis G. Socker  
Naval Research Laboratory, Washington, DC 20375

Joseph M. Davila  
NASA Goddard Space Flight Center, Greenbelt, MD 20771

Giancarlo Noci, Marco Romoli  
Università di Firenze  
I-50125 Firenze, Italy

Silvano Fineschi  
INAF - Osservatorio Astronomico di Torino  
I-10025 Torino, Italy

## ABSTRACT

The Advanced Spectroscopic and Coronagraphic Explorer (ASCE) was proposed in 2001 to NASA's Medium-Class Explorer (MIDEX) Program by the Smithsonian Astrophysical Observatory in collaboration with the Naval Research Laboratory, Goddard Space Flight Center, and the Italian Space Agency. It is one of four missions selected for Phase A study in 2002. ASCE is composed of three instrument units: an Advanced Ultraviolet Coronagraph Spectrograph (AUVCS), an Advanced Large Aperture Visible light Spectroscopic Coronagraph (ALASCO), and an Advanced Solar Disk Spectrometer (ASDS). ASCE makes use of a 13 m long boom that is extended on orbit and positions the external occulters of AUVCS and ALASCO nearly 15 m in front of their respective telescope mirrors. The optical design concepts for the instruments will be discussed.

**Keywords:** Solar Corona, UV Spectroscopy, Magnetic Fields, Coronagraphs, UV Optics, Polarization

## 1. INTRODUCTION

The Advanced Spectroscopic and Coronagraphic Explorer (ASCE) is a solar physics mission designed to answer the following questions:

- 1) What are the physical processes responsible for heating and accelerating the plasma components of the fast and slow solar wind?
- 2) How is sub-photospheric magnetic energy transported into the corona to be dissipated as heat and to drive mass flows?
- 3) How are Coronal Mass Ejections (CMEs) heated and accelerated, and what role do they play in the evolution of the solar magnetic field?

These questions will be answered using the tools of EUV spectroscopy and visible light polarimetry. Measurements will be made of profiles and intensities of emission lines from ions and atoms formed in the outer

layers of the solar atmosphere up to 10 solar radii (10  $R_{\odot}$ ) from Sun-center. Measurements will also be made of the polarization of visible light in the corona in order to determine the density of coronal electrons. Measurements made at high cadence will enable CMEs to be studied and followed from their initiation in the lower solar atmosphere to well into the extended solar corona.

ASCE was proposed in 2001 to NASA's Medium-class Explorer (MIDEX) Program by the Smithsonian Astrophysical Observatory, in collaboration with the Naval Research Laboratory, Goddard Space Flight Center, and the Italian Space Agency. It is one of four missions selected for Phase A study in 2002. The ASCE mission described here is a revised and improved version of that described by Gardner, et al.<sup>1</sup> The capabilities of the new instruments are roughly an order of magnitude greater than those of the UVCS, LASCO, and SUMER instruments on SOHO (Kohl et al.,<sup>2</sup> Brueckner et al.,<sup>3</sup> and Wilhelm et al.,<sup>4</sup> in Fleck et al.<sup>5</sup>).

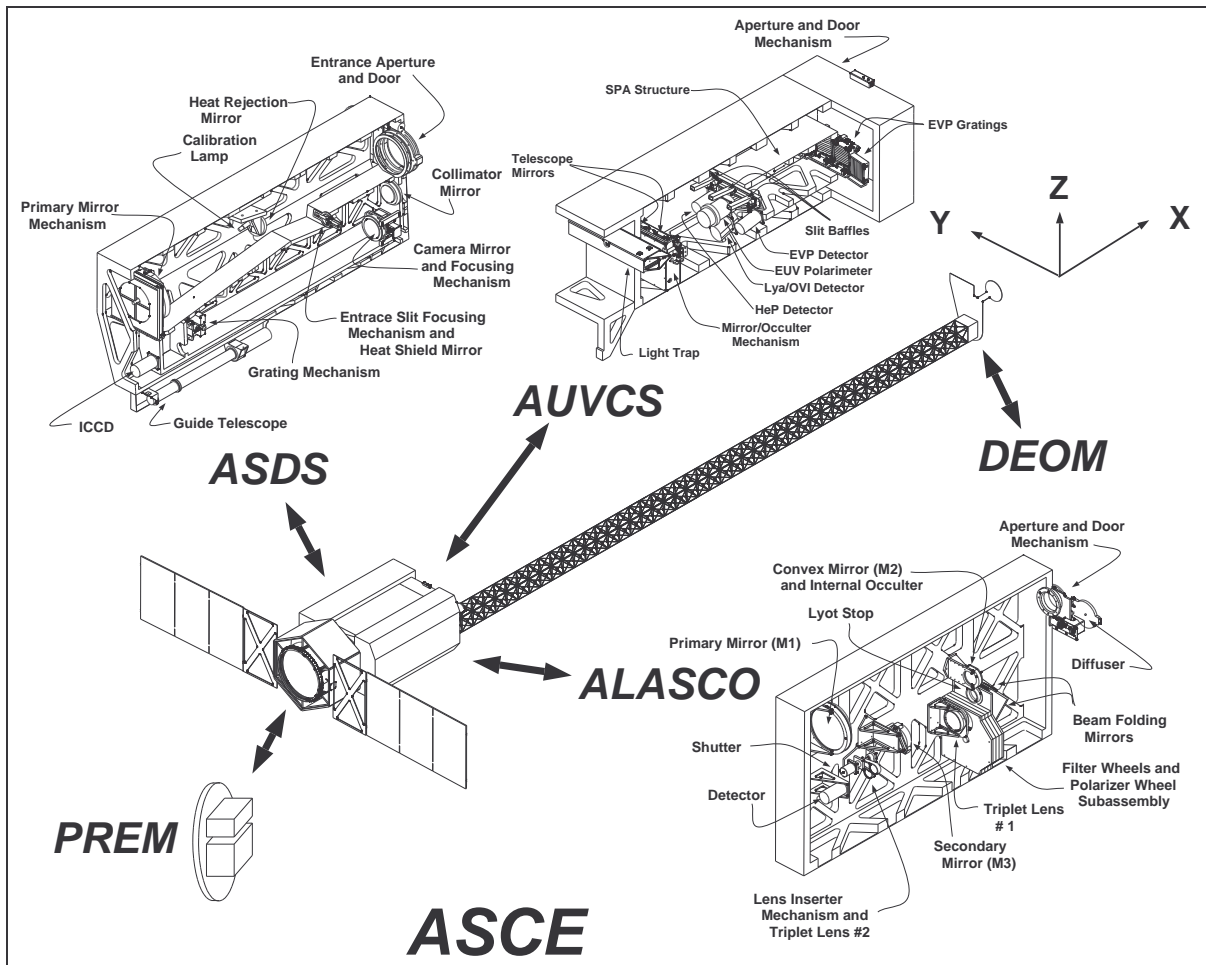


Figure 1. ASCE Payload. Details of the three instrument units, AUVCS, ASDS, and ALASCO, are shown. The remote external occulters are placed 13 m in front of the entrance apertures by the DEOM. The payload remote electronics module (PREM) is mounted onto one panel of the spacecraft bus.

The ASCE payload concept is shown in Figure 1. It is composed of three modules: the Spectroscopic, Polarimetric & Coronagraphic Module (SPCM), which is itself comprised of the three optical instrument units, an Advanced Ultraviolet Coronagraph Spectrograph (AUVCS), an Advanced Large Aperture visible light Spectroscopic Coronagraph (ALASCO), and an Advanced Solar Disk Spectrometer (ASDS); the Deployable

External Occulter Module (DEOM), which extends 13 m on orbit and positions the external occulters for the two coronagraphs; and the Payload Remote Electronics Module (PREM), which controls the science payload and communicates with the spacecraft bus.

In AUVCS there are multiple optical paths that enable high resolution line profile and intensity measurements over a wavelength range from below 30 nm to beyond 125 nm, spectro-polarimetry of the coronal hydrogen Lyman series lines, and measurement of the coronal electron temperature by direct measurement of the profile of the Thompson scattered H I 121.6 nm line. The ALASCO uses large aperture off-axis parabolic primary and secondary mirrors in a confocal configuration to minimize aberrations, coma, and astigmatism. It has the capability of measuring both the intensity and the polarization of visible coronal emission, both broad-band and in several distinct emission lines, at unprecedented spatial resolution. The ASDS uses a large aperture off-axis parabolic primary to feed an asymmetric plane grating spectrometer. High spectral resolution measurements in the EUV can be made anywhere on the solar disk with arc second spatial resolution. Further details of the optical designs are presented in the following sections.

## 2. AUVCS

The optical diagram for AUVCS is shown in Figure 2. It has three co-pivoting 750 mm focal length, off-axis parabolic, telescope mirrors that feed three normal incidence, Rowland circle spectrometers with Johnson-Onaka style grating rotation mechanisms. The plate scale is 0.28 arcsec/ $\mu\text{m}$ . The Helium Path (HeP) is for line profile and intensity measurements from 26 to 37 nm (2nd grating order) and from 48 to 74 nm (1st order), including grating rotation. Its range encompasses the He II line at 30.4 nm and the He I line at 58.4 nm. The grating is toric with primary and secondary radii of curvature of 750 mm and 736.1 mm, respectively. The ruling frequency of the grating is 3600 lines/mm; the reciprocal dispersion is 0.19 nm/mm in second order. Both the grating and telescope mirror are coated with a silicon-iridium multilayer to enhance normal incidence reflectivity near 30 nm. The EUV

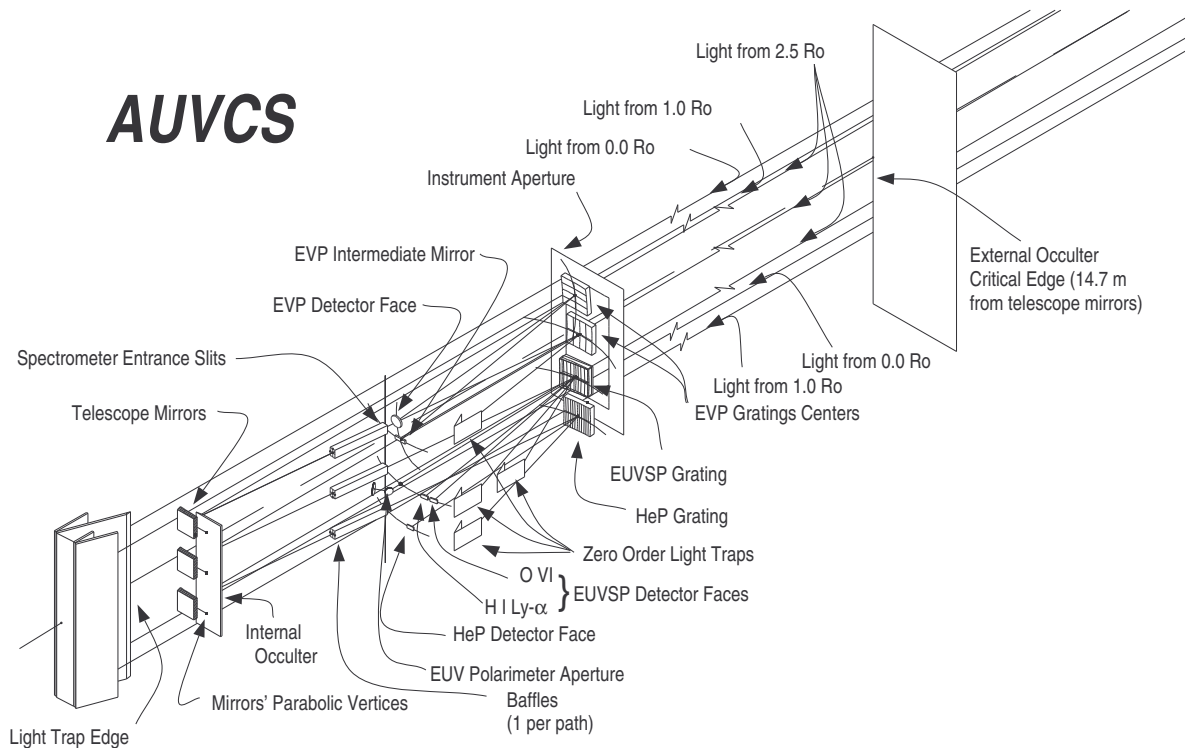


Figure 2. AUVCS Optical Diagram. The AUVCS has three primary optical paths, each of which is a Rowland circle spectrograph with toric gratings. See the text for detailed descriptions of each path.

Spectroscopy Path (EUVSP) is for line profile and intensity measurements from 38 to 75 nm (2nd order) and 75 to 150 nm (1st order), including grating rotation. Its range includes the important H I Ly- $\alpha$  line at 121.6 nm and the O VI doublet at 103.2 and 103.7 nm. Within this path is a “sub-path”, the EUV Polarimetry Path (EUVPP), which is intended for UV polarimetric measurements over the wavelength range 90 to 130 nm. It holds the promise of measuring anisotropic ion velocities and coronal magnetic fields (see Fineschi et al.,<sup>6</sup> this volume). The grating is toric with primary and secondary radii of curvature of 750 mm and 722.0 mm, respectively. The ruling frequency of the grating is 2400 lines/mm; the reciprocal dispersion is 0.56 nm/mm in first order. The telescope mirror is chemical vapor deposited (CVD) silicon carbide, and the grating is sputter-coated with silicon carbide. The Electron Velocity Distribution Path (EVP) is for measurements of the profiles of electron-scattered, coronal H I Ly- $\alpha$  radiation for direct determination of the velocity distributions of coronal electrons. It is a crossed-dispersion double spectrograph designed to minimize in-band stray light. The concept has been previously described.<sup>1</sup> The gratings are toric with primary and secondary radii of curvature of 750 mm and 744.1 mm, respectively. The ruling frequency of the gratings is 1200 lines/mm. The optical coatings are lithium fluoride over aluminum.

The detectors for AUVCS are intensified CCDs (ICCDs) that operate in photon counting mode.<sup>7</sup> Details about each detector are provided in Table 1, and an example of the design concept is illustrated in Figure 3. The

Table 1. Intensified CCD Detector Characteristics.

Path or Channel	HeP	EUVSP	EVP	ASDS
Mode	Photon Counting	Photon Counting	Photon Counting	Imaging
MCP (mm)	25 $\phi$	15 x 60 (a)	40 $\phi$	25 $\phi$ (b)
CCD	Atmel THX7887A			E2V CCD47-20
Number of CCDs; CCD pixels used on each	1; 1000x500	2; 1000x500	1; 1024x1024	2; 815x815
CCD pixel size ( $\mu\text{m}$ )	14	14	14	13.5
Readout noise; Full well	250000	250000	250000	100000
Operating Temperature	ambient	ambient	ambient	-40 C
MCP Photosensitive Area [mm x mm]	20 x 10	2 x 20 x 10	28 x 28	22 x 11
Fiber Optic Taper; MCP:CCD	1:0.7	2 @ 1:0.7	1:0.7	1:1
Centroiding	$\frac{1}{2}$ pixel	$\frac{1}{2}$ pixel	$\frac{1}{2}$ pixel	none
On-chip binning	no	no	4 x 4	No
FWHM Effective Pixel (EP) Size [ $\mu\text{m}$ ](c)	10	10	110	21
Maximum frame rate [ $\text{s}^{-1}$ ]	120	2 x 120	120	n.a.
Local Count Rate @ 10% loss [ $\text{EP}^{-1}\text{-s}^{-1}$ ]	0.6	1.0	70	n.a.
Dark Rate [ $\text{EP}^{-1}\text{-s}^{-1}$ ]	$< 1 \times 10^{-6}$	$< 1 \times 10^{-6}$	$< 1 \times 10^{-5}$	$10 \text{ e}^-$ at 1 MHz
QE of KBr @ $\lambda$ [nm]	0.35 @ 30	0.42 @ 103; 0.28 @ 122		0.42 @ 103

(a) One MCP chevron; two fiber optic tapers and two CCDs.

(b) One MCP; one fiber optic coupler and two CCDs; E2V CCD47-20 is back-thinned version.

(c) FWHM of the detector response to a point source at the surface of the MCP. For the imaging detector this was calculated as an inverse Fourier transform of the modulation transfer function.

intensifier portion of each detector consists of a KBr coated chevron microchannel plate (MCP) pair. Electrons leaving the back of the MCPs are accelerated by  $\sim 5000$  V toward an aluminum film that overcoats a short-persistence phosphor on a fiberoptic faceplate. Light flashes from the phosphor are coupled through the faceplate and a subsequent fiber optic taper to one (for HeP and EVP) or two (for EUVSP) 1024x1024 CCDs. The light flashes, spread over several pixels, are converted to electrons in the CCD. The CCD is rapidly read out and the output processed in a centroider (implemented in hardware) that determines the location of the peak of each “flash” to  $1/2$  of a CCD pixel. A memory address corresponding to the coordinates of that centroid is incremented. The MCPs are operated at a gain of  $10^4$  to  $10^5$ , which is relatively low compared to other photon counting detectors. MCP aging effects (gain loss with accumulated photon dose) are expected to be negligible.

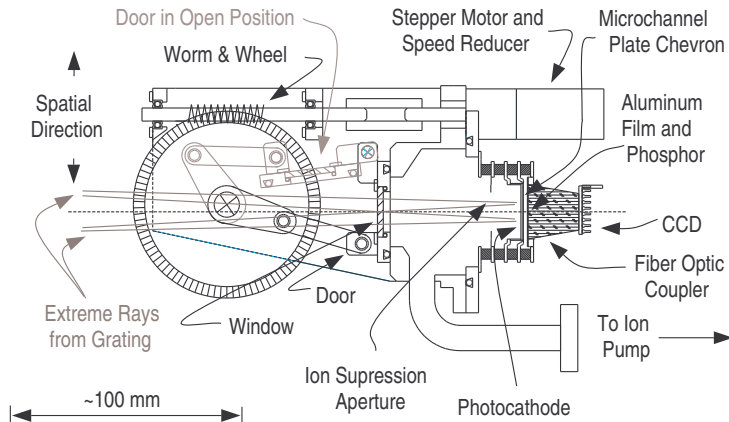


Figure 3. ICCD Design Concept. See the text for operating details.

### 3. ASDS

The ASDS optical diagram is shown in Figure 4. It is an off-axis parabolic telescope feeding an asymmetric Czerny-Turner spectrograph. It is designed for very high spatial, spectral, and temporal resolution spectroscopy of the solar disk, chromosphere, transition region, and corona to 1.5  $R_{\odot}$ . The spectrometer design utilizes a plane grating and so provides stigmatic imaging, with the grating rotation, over a wide spectral range; the asymmetric design provides magnification of the

entrance slit image by 3.6 for sub-arcsec imaging with  $13.5 \mu\text{m}$  detector pixels ( $21 \mu\text{m}$  resolution elements). The off-axis parabolic telescope mirror has a 2-D slew mechanism together with tip and tilt in order to view the entire FOV without aberrations. The detector system is a SERTS based ICCD<sup>8</sup> and operates in camera mode; performance details are listed in Table 1 above.

The primary, collimator, and camera mirrors are all CVD SiC. The grating has a ruling frequency of 1800 lines/mm and provides a reciprocal dispersion of 0.30 nm/mm. It is coated with sputtered SiC. The spectrometer

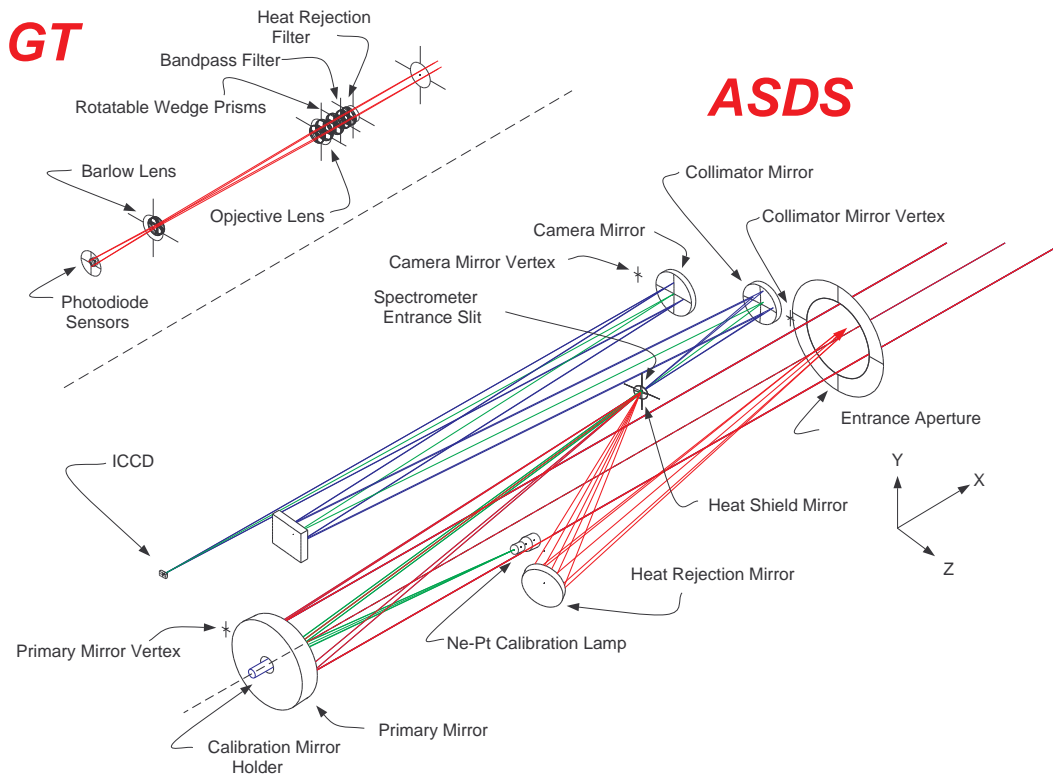


Figure 4. ASDS Optical Diagram. Light from the solar disk is focused onto the entrance slit of an asymmetric Czerny-Turner spectrograph. Spacecraft alignment to disk center is controlled by a guide telescope (GT), shown in the upper right, the design of which is taken from the TRACE mission.

entrance slit is 1 arcsec wide by 7 arcmin long. Mechanisms on the entrance slit and camera mirror are used to achieve optimum focus on orbit. The mechanism on the primary mirror allows a rapid 2-D raster (1 arcsec steps with placement accuracy 0.5 arcsec) of a 7 arcmin x 7 arcmin region. A slower slew mechanism allows the 7 x 7 arcmin region to be centered anywhere from Sun-center to 1.3  $R_o$ . The spacecraft guide telescope, which provides sub-arcsec spacecraft pointing, is rigidly attached to and coaligned with the ASDS optical bench. A mirrored baffle in front of the entrance-slit refocuses and directs most of the solar radiation reflected from the primary mirror toward a secondary mirror that then reflects it back out the entrance aperture. A Ne-Pt hollow cathode lamp provides wavelength calibration lines, which can be used to directly measure Doppler shifts.

#### 4. ALASCO

The ALASCO optical design, shown in Figure 5, is designed for visible light polarimetry and intensity measurements over an annular field of view (FOV) from 1.1 to 10.3  $R_o$ . The entrance aperture is fully in the umbra of the 14.8 m distant external occulter providing an enormous advantage in straylight rejection over previous visible light coronagraphs. The optical system has an externally and internally occulted telescope composed of a set of three mirrors, two that are off-axis parabolooids and one that is convex-spherical, to present a collimated coronal beam to a polarimeter composed of three selectable fixed linear polarizers and selectable band-pass filters. Light passing through the polarimeter is imaged using a system of lenses onto a 4096 x 4096 pixel CCD camera. The lens system has selectable elements and allows the full 1.1 to 10.3  $R_o$  FOV to be imaged at a scale of 3.5 arcsec per CCD pixel, or a reduced 1.1 to 4.3  $R_o$  FOV to be imaged at a scale of 2 arcsec per pixel. This provides resolution elements of 2 arcsec down to 1.8  $R_o$  where diffraction begins to limit the resolution in

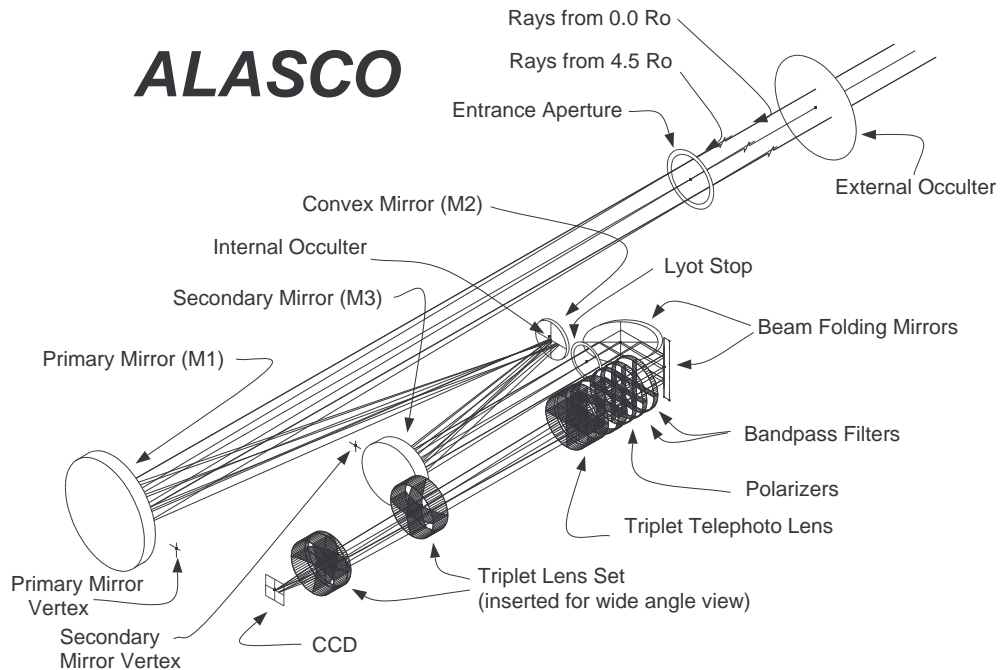


Figure 5. ALASCO Optical System. Light from the corona is collected by the primary mirror (M1) and brought to a focus in front of the convex mirror (M2). The image of the external occulter is blocked by the internal occulter, which is positioned immediately in front of M2. The light reflected from M2 is then recollimated by the secondary mirror (M3) and passed through an aperture, the Lyot stop, which is located at the position of the image formed by M2 and M3 of M1. After two 90 degree bends, the coronal light passes through selectable filters and/or polarizers and is finally imaged onto the CCD detector by two sets of triplet lenses. The second triplet can be inserted into the optical path to allow a larger field of view.



the radial direction. The large diameter primary mirror allows for a small diffraction limit and ensures a large effective area, which in turn allows sub-second exposure times and a complete set of broadband polarization measurements in less than one minute. In addition to broadband polarimetry near 590 nm, an additional set of 6 narrow band filters allows on and off-band intensity measurements and polarimetry at 530.3 nm [Fe XIV], 637.4 nm [Fe X], and 656.3 nm [H  $\alpha$ ].

## 5. SUMMARY

The optical designs of ASCE draw principally on the designs of the UVCS and LASCO instruments on SOHO. External occulters positioned by the DEOM many meters distant from the respective primary mirrors allow for much larger unvignetted telescope areas and corresponding increases in effective area, and, for ALASCO in particular, a major decrease in the diffraction limit. The distant external occulters also provide reduced stray light levels as compared to previous EUV and visible light coronagraphs. When coupled with the ASDS, a 1 arcsec effective pixel EUV solar disk telescope-spectrometer, it becomes possible to follow solar events and particle acceleration from the photosphere into the extended corona.

The mission was proposed to NASA's MIDEX program in 2001 and, with three other missions, was selected for Phase A study in 2002. The concept study reports are due in October of 2002. Selection by NASA for the continuation of two missions is planned in the Spring of 2003.

## ACKNOWLEDGEMENTS

This work was supported by NASA contract No. NAS5-02093 to the Smithsonian Astrophysical Observatory.

## REFERENCES

1. L.D. Gardner, J.L. Kohl, S. Cranmer, S. Fineschi, L. Golub, J. Raymond, P.L. Smith, L. Strachan, R. Howard, D. Moses, D. Socker, D. Wang, R.R. Fisher, J. Davila, C. St. Cyr, G. Noci, M. Romoli, G. Tondello, G. Naletto, P. Nicolosi, L. Poletto, "The Advanced Solar Coronal Explorer Mission (ASCE)," *Proc. SPIE* **3764**, 134, 1999.
2. J.L. Kohl, R. Esser, L.D. Gardner, S. Habbal, P.S. Daigneau, E. Dennis, G.U. Nystrom, A. Panasyuk, J.C. Raymond, P.L. Smith, L. Strachan, A. Van Ballegooijen, G. Noci, S. Fineschi, M. Romoli, A. Ciaravella, A. Modigliani, M.C.E. Huber, E. Antonucci, C. Benna, S. Giordano, G. Tondello, P. Nicolosi, G. Naletto, C. Pernechele, D. Spadaro, G. Poletto, S. Livi, O. Von Der Luhe, J. Geiss, J.G. Timothy, G. Gloeckler, A. Allegra, G. Basile, R. Brusa, B. Wood, O.H.W. Siegmund, W. Fowler, R. Fisher, and M. Jhabvala, "The Ultraviolet Coronagraph Spectrometer for the Solar and Heliospheric Observatory," *Solar Phys.* **162**, 313, 1995.
3. G.E. Brueckner, R.A. Howard, M.J. Koomen, C.M. Korendyke, D.J. Michels, J.D. Moses, D.G. Socker, K.P. Dere, P.L. Lamy, A. Llebaria, M.V. Bout, R. Schwenn, G.M. Simnet, D.K. Bedford, and C.J. Eyles, "The Large Angle Spectroscopic Coronagraph," *Solar Phys.* **162**, 357, 1995.
4. K. Wilhelm, W. Curdt, E. Marsch, U. Schuele, P. Lemaire, A. Gabriel, J.-C. Vial, M. Grewing, M.C.E. Huber, S.D. Jordan, A.I. Poland, R.J. Thomas, M. Kuehne, J.G. Timothy, D.M. Hassler, and O.H.W. Siegmund, "SUMER- Solar Ultraviolet Measurements of Emitted Radiation," *Solar Phys.* **162**, 189, 1995.
5. B. Fleck, V. Domingo, and A.I. Poland, ed., *The SOHO Mission*, Reprinted from *Solar Phys.* **162**, 1, Kluwer Academic Publishers, Dordrecht, The Netherlands, 1995.
6. S. Fineschi, J.L. Kohl, L.D. Gardner, and M. Romoli, "Spectro-polarimetry of the EUV-UV Solar Corona," *Proc. SPIE* **4843** (this volume), 2002.
7. T.J. Norton, P.F. Morrissey, P. Haas, L.J. Payne, J. Carbonne, and R.A. Kimble, "Photon-counting intensified random-access charge injection device," *Proc. SPIE* **3764**, 234, 1999.
8. L.P. Payne, and J.P. Haas, "General Purpose Solid State Camera for SERTS," *Proc. SPIE* **2804**, 118, 1996.